Purinergic Signalling (2013) 9:433–449
DOI 10.1007/s11302-013-9364-5

ORIGINAL ARTICLE

$A_1R–A_{2A}R$ heteromers coupled to G_s and $G_{i/0}$ proteins modulate GABA transport into astrocytes

Sofia Cristóvão-Ferreira · Gemma Navarro · Marc Brugarolas · Kamil Pérez-Capote · Sandra H. Vaz · Giorgia Fattorini · Fiorenzo Conti · Carmen Lluis · Joaquim A. Ribeiro · Peter J. McCormick · Vicent Casadó · Rafael Franco · Ana M. Sebastião

Received: 27 February 2013 / Accepted: 22 April 2013 / Published online: 10 May 2013

Abstract Astrocytes play a key role in modulating synaptic transmission by controlling extracellular gamma-aminobutyric acid (GABA) levels via GAT-1 and GAT-3 GABA transporters (GATs). Using primary cultures of rat astrocytes, we show here that a further level of regulation of GABA uptake occurs via modulation of the GATs by the adenosine A_1 (A_1R) and A_{2A} ($A_{2A}R$) receptors. This regulation occurs through $A_1R–A_{2A}R$ heteromers that signal via two different G proteins, G_s and $G_{i/0}$, and either enhances ($A_{2A}R$) or inhibits (A_1R) GABA uptake. These results provide novel mechanistic insight into how GPCR heteromers signal. Furthermore, we uncover a previously unknown mechanism where adenosine, in a concentration-dependent manner, acts via a heterocomplex of adenosine receptors in astrocytes to significantly contribute to neurotransmission at the tripartite (neuron–glia–neuron) synapse.

Keywords Adenosine heteromers · G protein coupling · GABA transporters · Astrocytes

Introduction

Astrocytes modulate synaptic transmission as they can release and uptake neurotransmitters [1] and, therefore, fine-tune the balance between excitation and inhibition. Gamma-aminobutyric acid (GABA) is the main inhibitory neurotransmitter in the central nervous system, where it plays a crucial role in the control of excitability [2], plasticity [3], and network synchronization [4]. These actions depend on changes in the extracellular concentrations of GABA, which are under control of GABA transporters (GATs) expressed both in neurons and astrocytes [5, 6]. Cortical astrocytes express GAT-1 and GAT-3 subtypes and it has been estimated that approximately 20 % of extracellular GABA may be taken up into astrocytes [7].

Astrocytes release large amounts of ATP, which is then hydrolysed into adenosine by the action of ectonucleotidases [see, e.g., 1]. Extracellular adenosine operates through G-

S. Cristóvão-Ferreira · S. H. Vaz · J. A. Ribeiro · A. M. Sebastião (✉)
Institute of Pharmacology and Neurosciences, Faculty of Medicine, University of Lisbon, Av. Professor Egas Moniz, Edificio Egas Moniz, 1649-028 Lisbon, Portugal
e-mail: anaseb@fm.ul.pt

S. Cristóvão-Ferreira · S. H. Vaz · J. A. Ribeiro · A. M. Sebastião
Unit of Neurosciences, Institute of Molecular Medicine, University of Lisbon, Av. Professor Egas Moniz, Edificio Egas Moniz, 1649-028 Lisbon, Portugal

G. Navarro · M. Brugarolas · K. Pérez-Capote · C. Lluis · P. J. McCormick · V. Casadó · R. Franco
Centro de Investigación Biomédica en Red sobre Enfermedades Neurodegenerativas (CIBERNED), University of Barcelona, Barcelona, Spain

G. Navarro · M. Brugarolas · K. Pérez-Capote · C. Lluis · P. J. McCormick · V. Casadó · R. Franco
Department of Biochemistry and Molecular Biology, Faculty of Biology, University of Barcelona, Barcelona, Spain

G. Fattorini · F. Conti
Department of Neuroscience, Università Politecnica delle Marche, Ancona, Italy

G. Fattorini · F. Conti
Center for Neurobiology of Aging, INRCA IRCCS, Ancona, Italy

F. Conti
Fondazione di Medicina Molecolare, Università Politecnica delle Marche, Ancona, Italy

R. Franco
Laboratory of Cell and Molecular Neuropharmacology, Neurosciences Division, Centro de Investigación Médica Aplicada (CIMA), University of Navarra, Pamplona, Spain

protein coupled receptors. In the case of neural cells, the A_1 (A_1R) and A_{2A} ($A_{2A}R$) receptor subtypes are those that are most likely activated by basal levels of extracellular adenosine. The A_1R is often inhibitory and couple to $G_{i/0}$ proteins, while the $A_{2A}R$ is usually coupled to G_s proteins, enhancing cAMP accumulation and PKA activity [see, e.g., 8]. A_1R and $A_{2A}R$ receptors may closely interact in such a way that activation of $A_{2A}R$ receptors can lead to inhibition of A_1R-mediated responses [9–11]. Some interactions may occur at the functional and transducing system levels [see, e.g., 12] but energy transfer assays in the form of bioluminescence resonance energy transfer (BRET) and fluorescence resonance energy transfer (FRET) have identified the presence of A_1R–$A_{2A}R$ heteromers in immortalized transfected cells [13]. In addition, the A_1R–$A_{2A}R$ heteromers have been identified in presynaptic membranes via co-immunoprecipitation experiments and it has been shown that these heteromers modulate glutamate release from presynaptic nerve terminals [13]. Taken together, these data strongly suggest a putative role of A_1R–$A_{2A}R$ heteromers in neurons. However, direct evidence for A_1R–$A_{2A}R$ heteromerization in neural cells is, still lacking.

Due to the role of astrocytes in overall GABA transport, a first aim of the present work was to clarify whether A_1R and $A_{2A}R$ modulate GAT-1- and/or GAT-3-mediated GABA transport into astrocytes. We detected a tight interaction between A_1R and $A_{2A}R$, including evidence for cross-antagonism, a biochemical property often demonstrated for receptor heteromers [14]. In addition, we found A_1R–$A_{2A}R$ receptor heteromers in astrocytes. We found these heteromers couple to two different G proteins, G_s and $G_{i/0}$, both regulating GABA transport in an opposite way, with the A_1R protomer mediating inhibition of GABA transport and the $A_{2A}R$ protomer mediating facilitation of GABA transport into astrocytes. This A_1R–$A_{2A}R$ receptor functional unit may, therefore, operate as a dual amplifier to control ambient GABA levels at synapses.

Material and methods

All animal procedures were carried out according to the European Community Guidelines for Animal Care (European Communities Council Directive-86/609/EEC). Throughout the underlying experimental work, care was taken to minimize the number of animals used.

Cell lines and primary astrocytic cultures

The astrocytes were prepared from the cortex of newborn (P1–P2) Wistar rats of either sex. Briefly, rat brains were dissected out of pups and cortex were isolated and the meninges and white matter were removed. Cortex was dissociated gently by grinding in Dulbecco's modified Eagle's medium (DMEM) medium, filtered through a cell strainer and centrifuged at 200 g for 10 min. The pellet was resuspendend in DMEM and filtered. The cells were then seeded and kept for 4 weeks in DMEM containing 10 % (*v*/*v*) fetal bovine serum with antibiotic (Sigma) in a humidified atmosphere (5 % CO2) at 37 °C. CHO cells clones expressing A_1R, $A_{2A}R$ or both were obtained and cultured as previously indicated [15]. HEK-293T cells were grown in DMEM (Gibco) supplemented with 2 mM L-glutamine, 100 U/ml penicillin/streptomycin, and 5 % (*v*/*v*) heat inactivated fetal bovine serum (all supplements were from Invitrogen, Paisley, Scotland, UK). Cells were maintained at 37 °C in an atmosphere of 5 % CO_2, and were passaged when they were 80–90 % confluent, i.e., approximately twice a week.

[^{3}H]GABA uptake

Assays were performed in a nonsupplemented low-glucose DMEM. Astrocytes were preincubated with adenosine deaminase (ADA) for 15 min before adding the test drugs, except when otherwise indicated; test drugs were added and incubation continued for further 20 min. GABA uptake was initiated by the addition of 30 μM [^{3}H]GABA (except otherwise specified). Transport was stopped after 40 s with 2 ml of ice-cold PBS. The amount of [^{3}H]GABA taken up by astrocytes was quantified by liquid scintillation counting. GAT-1- and GAT-3-mediated transports were calculated through the subtraction of the amount of GABA taken up in the presence of the specific blocker of GAT-1, SKF 89976A (20 μM) or the specific blocker of GAT-3, SNAP 5114 (40 μM), respectively, to the total transport.

Expression vectors and cell transfections

The human cDNAs for $A_{2A}R$ and A_1R, cloned into pcDNA3.1 were amplified without their stop codons using sense and antisense primers harboring unique EcoRI and BamHI sites to clone $A_{2A}R$ in RLuc vector and EcoRI and KpnI to clone A_1R in EYFP vector. The amplified fragments were subcloned to be in-frame into restriction sites of pcDNA3.1RLuc (p*RLuc*-N1 PerkinElmer, Wellesley, MA, USA) and pEYFP-N1 (enhanced yellow variant of GFP; Clontech, Heidelberg, Germany) to give the plasmids that express A_1R or $A_{2A}R$ fused to RLuc or YFP on the C-terminal end of the receptor ($A_{2A}R$–RLuc and A_1R–YFP). The cDNA encoding the serotonin $5HT_{2B}$-YFP fusion protein was kindly provided by Dr. Irma Nardi (University of Pisa, Italy). Expression of constructs was tested by confocal microscopy and the receptor functionality by second messengers, ERK1/2 phosphorylation and cAMP production as described previously [16, 17]. HEK-293T cells or 2-week

cultured primary astrocytes growing in six-well dishes were transiently transfected with the corresponding fusion protein cDNA by the polyethylenimine (PEI, Sigma) method. Cells were incubated (4 h) with the corresponding cDNA together with PEI (5.47 mM in nitrogen residues) and 150 mM NaCl in a serum-starved medium. After 4 h, the medium was changed to a fresh complete culture medium. Forty-eight hours after transfection, cells were washed twice in quick succession in HBSS with 10 mM glucose, detached, and resuspended in the same buffer containing 1 mM EDTA. To control the cell number, sample protein concentration was determined using a Bradford assay kit (Bio-Rad, Munich, Germany) using bovine serum albumin dilutions as standards. Cell suspension (20 μg of protein) was distributed into 96-well microplates; black plates with a transparent bottom were used for fluorescence determinations, while white plates were used for BRET experiments.

Immunocytochemistry

For immunocytochemistry with primary cultures of astrocytes, cell were incubated with ADA (1 U/ml) for 15 min, fixed in 4 % paraformaldehyde for 20 min, and washed with PBS containing 20 mM glycine (buffer A) to quench the aldehyde groups. Then, after permeabilization with 10 % normal goat serum containing 0.3 % Triton X-100 for 5 min, cells were treated with PBS containing 1 % bovine serum albumin. After 1 h at room temperature, astrocytes were incubated with antibodies rabbit anti-GAT-1 (1:100; kindly provided by N. Brecha, UCLA) and mouse anti-GFAP (1:800; Sigma) or rabbit anti-GAT-3 (1:200; kindly provided by N. Brecha, UCLA) and mouse anti-GFAP (1:800; Sigma) antibodies for 3 h at RT. After washes, astrocytes were stained with the secondary antibodies for 1.5 h at RT FITC-conjugated anti-rabbit IgG (FI-1000) and TRITC-conjugated anti-mouse IgG (T-2762; Vector Laboratories). Dishes were then mounted, air-dried, and coverslipped using Vectashield mounting medium (H-1000; Vector). For immunocytochemistry with transiently transfected HEK-293T cells, cells treated as indicated in figure legends, were fixed and permeabilized as indicated above. Cells expressing $A_{2A}R$–RLuc were labeled with the primary mouse monoclonal anti-*RLuc* antibody (1:100, Chemicon) for 1 h, washed, and stained with the secondary antibody Cy3 Donkey anti-mouse (1:100, Jackson Immunoresearch Laboratories, Baltimore, PA, USA). A_1R–YFP was detected by its fluorescence properties. Samples were rinsed and observed in a Leica SP2 confocal microscope (Leica Microsystems, Mannheim, Germany).

Western blot

For A_1R and $A_{2A}R$ detection, primary astrocytes were rinsed with ice-cold phosphate-buffered saline and lysed in 8 M urea, 2 % SDS, 100 mM DTT, 375 mM Tris, and pH 6.8 by heating to 37 °C for 2 h and resolved by SDS-PAGE. Proteins were transferred to poly(vinylidene) difluoride membranes using a semidry transfer system and immunoblotted with the primary antibodies mouse anti-A_{2A} antibody (1:1,000; Upstate) or rabbit anti-A_1 antibody (1:1,000; ABR05). The blots were then incubated with a secondary horseradish peroxidase-conjugated rabbit anti-mouse IgG antibody (1:2,500) or goat anti-rabbit IgG antibody (1:60,000). The immunoreactive bands were developed using a chemiluminescent detection kit. For GAT-1 and GAT-3 detection, the primary cultures of astrocytes were mechanically lysed with sucrose-containing buffer (sucrose 0.32 M, EDTA 1 mM, HEPES 10 mM, bovine serum albumin 1 mg/ml, pH 7.4). To clarify, the homogenate was centrifuged (13,000 g, 10 min) and the supernatant was collected. After denaturation (by Laemmli buffer heated at 95 °C for 5 min), the extracts were run on a 10 % acrylamide gel. Protein was transferred to a nitrocellulose membrane by electroblotting. Western blotting was performed using the anti-GAT-1 (1:100) and anti-GAT-3(1:200), kindly provided by N. Brecha, UCLA. After exposure to secondary antibody (peroxidase anti-rabbit (1:250) Vector; Burlingame, CA, USA), bands were visualized by BioRad Chemidoc and Quantity One software.

BRET assays

Primary astrocytes or HEK-293T cells were transiently co-transfected with a constant amount of the cDNA encoding for receptors fused to RLuc, and with increasingly amounts of the cDNA corresponding to receptors fused to YFP (see figure legends). To quantify receptor-YFP expression cells (20 μg protein) were distributed in 96-well microplates (black plates with a transparent bottom) and fluorescence was read in a Fluo Star Optima Fluorimeter (BMG Labtechnologies, Offenburg, Germany) equipped with a high-energy xenon flash lamp, using a 10-nm bandwidth excitation filter at 400 nm reading. Receptor fluorescence expression was determined as fluorescence of the sample minus the fluorescence of cells expressing the BRET donor alone. For BRET measurements, the equivalent of 20 μg of cell suspension were distributed in 96-well microplates (Corning 3600, white plates; Sigma) and 5 μM coelenterazine H (Molecular Probes, Eugene, OR, USA) was added. After 1 min of adding coelenterazine H, the readings were collected using a Mithras LB 940 that allows the integration of the signals detected in the short wavelength filter at 485 nm (440–500 nm) and the long wavelength filter at 530 nm (510–590 nm). To quantify receptor-RLuc expression, luminescence readings were also performed after 10 min of adding 5 μM coelenterazine H. The net BRET is defined as [(long wavelength emission)/(short wavelength emission)]−Cf where Cf corresponds to [(long wavelength emission)/(short wavelength emission)] for the

donor construct expressed alone in the same experiment. BRET is expressed as mili-BRET units, mBU, (net BRET × 1,000).

Radioligand binding experiments

Four-week cultured primary astrocytes were disrupted with a polytron homogenizer (PTA 20 TS rotor, setting 3; Kinematica, Basel, Switzerland) for three 5-s periods in 10 volumes of 50 mM Tris–HCl buffer, pH 7.4 containing a proteinase inhibitor cocktail (Sigma, St. Louis, MO, USA). Cell debris was eliminated by centrifugation at 1,000×*g*, and membranes were obtained by centrifugation at 105,000 g (40 min, 4 °C). Pellet was resuspended and recentrifuged under the same conditions. Membranes were stored at −80 °C and were washed once more as described above and resuspended in 50 mM Tris–HCl buffer for immediate use. Competition experiments were performed by incubating (120 min) membranes (0.18 mg protein/ml) at 25 °C in 50 mM Tris–HCl buffer, pH 7.4, containing 10 mM $MgCl_2$ and 0.2 U/ml adenosine deaminase with 0.8 nM ^{3}H-labeled *R*-phenylisopropyladenosine ([^{3}H]R–PIA) in the absence or presence of increasing concentrations of CGS 21680 or SCH 58261. Nonspecific binding was determined in the presence of 10 μM *R*-phenylisopropyladenosine (R-PIA). Free and membrane-bound ligand were separated by rapid filtration of 500 μl aliquots in a cell harvester (Brandel, Gaithersburg, MD, USA) through Whatman GF/C filters embedded in 0.3 % polyethylenimine that were subsequently washed for 5 s with 5 ml of ice-cold Tris–HCl buffer. The filters were incubated with 10 ml of Ecoscint H scintillation cocktail (National Diagnostics, Atlanta, GA, USA) overnight at room temperature and radioactivity counts were determined using a Tri-Carb 1600 scintillation counter (PerkinElmer, Boston, MA, USA) with an efficiency of 62 % [18]. Radioligand displacement curves were analyzed by nonlinear regression using commercial program GRAFIT (Erithacus Software, Surrey, UK) as indicated previously [13].

[^{35}S]GTP-γ-S assay

For quantification of GTP activity, GDP (10 μM) was added to the primary astrocytic membranes and incubated on ice for 10 min. Membranes were incubated at 37 °C for 10 min with ADA (1 U/ml) before the addition of DPCPX or SCH 58261 antagonists and after 10 min, the [^{35}S]GTP-γ-S (1 nM) and the tested drugs were added and incubate for 30 min at 37 °C. Membranes were collected and solubilised and the antibodies were added: 5 μg of anti-$G_{\alpha\ i\text{-}3}$ (sc-262), 10 μg of anti-$G_{\alpha\ S}$ (sc-6766), or 10 μg of anti-$G_{\alpha\ q/11}$ (sc-392), for G_i, G_S and $G_{q/11}$ studies, respectively. After an overnight incubation at 4 °C, protein G-sepharose was added and incubated for 90 min at 4 °C. The sepharose was washed five times with the solubilisation buffer and the incorporation of [^{35}S]GTP-γ-S was measured by liquid scintillation.

Biotinylation assays

Astrocytes were incubated for 30 min without (control) or with the agonists or antagonist of A_1R or A_{2A}R or both. When antagonist and agonist were tested together, the antagonist was added 15 min before. After, they were incubated for 1 h with 1 mg/ml Sulfo-NHS-LC-biotin (Pierce, Rockford, IL, USA) in PBS-Ca^{2+}-Mg^{2+} with gentle shaking. The biotin reaction was quenched with 100 mM glycine. The astrocytes were mechanically lysed with sucrose-containing buffer and centrifuged at 14,000×*g* for 10 min at 4 °C. Biotinylated surface proteins were immunoprecipitated with avidin beads (Pierce) overnight at 4 °C and centrifuged at 14,000×*g* for 10 min at 4 °C. Avidin beads were pelleted by centrifugation at 3,000×*g*, 4 °C, 10 min. Pellet (biotinylated fraction) was separated from the supernatant (intracellular fraction). Then, 150 μl of Laemmli buffer [70 mM Tris–HCl pH 6.8, 6 % glycerol, 2 % sodium dodecyl sulfate, 120 mM DTT (DLDithiothreitol), 0.0024 % bromophenol blue] was added to the pellet and heated to 37 °C for 30 min. The avidin beads were removed by filtration. Equal volumes of each sample was loaded on gel and resolved by SDS-PAGE.

CellKey label-free assays

The CellKey system provides a universal, label-free, cell-based assay platform that uses cellular dielectric spectroscopy to measure endogenous and transfected receptor activation in real time in live cells [19]. Changes in the complex impedance (ΔZ or dZ) of a cell monolayer in response to receptor stimulation were measured. Impedance (Z) is defined by the ratio of voltage to current as described by Ohm's law ($Z = V/I$). CHO cell clones stably expressing A_1R, A_{2A}R or both were grown to confluence in a CellKey Standard 96-well microplate that contains electrodes at the bottom of each well. For untreated cells or for cells preincubated (overnight at 37 °C) with Pertussis toxin (PTx; 10 ng/ml) or cholera toxin (ChTx; 100 ng/ml), medium was replaced by HBSS buffer (Gibco) supplemented with 20 mM HEPES 30 min prior to running the cell equilibration protocol. A baseline was recorded for 5 min and then cells were treated with the A_1R agonist CPA (10 nM) or with the A_{2A}R agonist CGS 21680 (10 nM) and data was acquired for the following 10 min. To calculate the impedance, small voltages at 24 different measurement frequencies were applied to treated or nontreated cells. At low frequencies, extracellular currents (iec) that pass around individual cells in the layer were induced. At high frequencies, transcellular currents (itc) that penetrate the cellular membrane were induced and the ratio of the applied

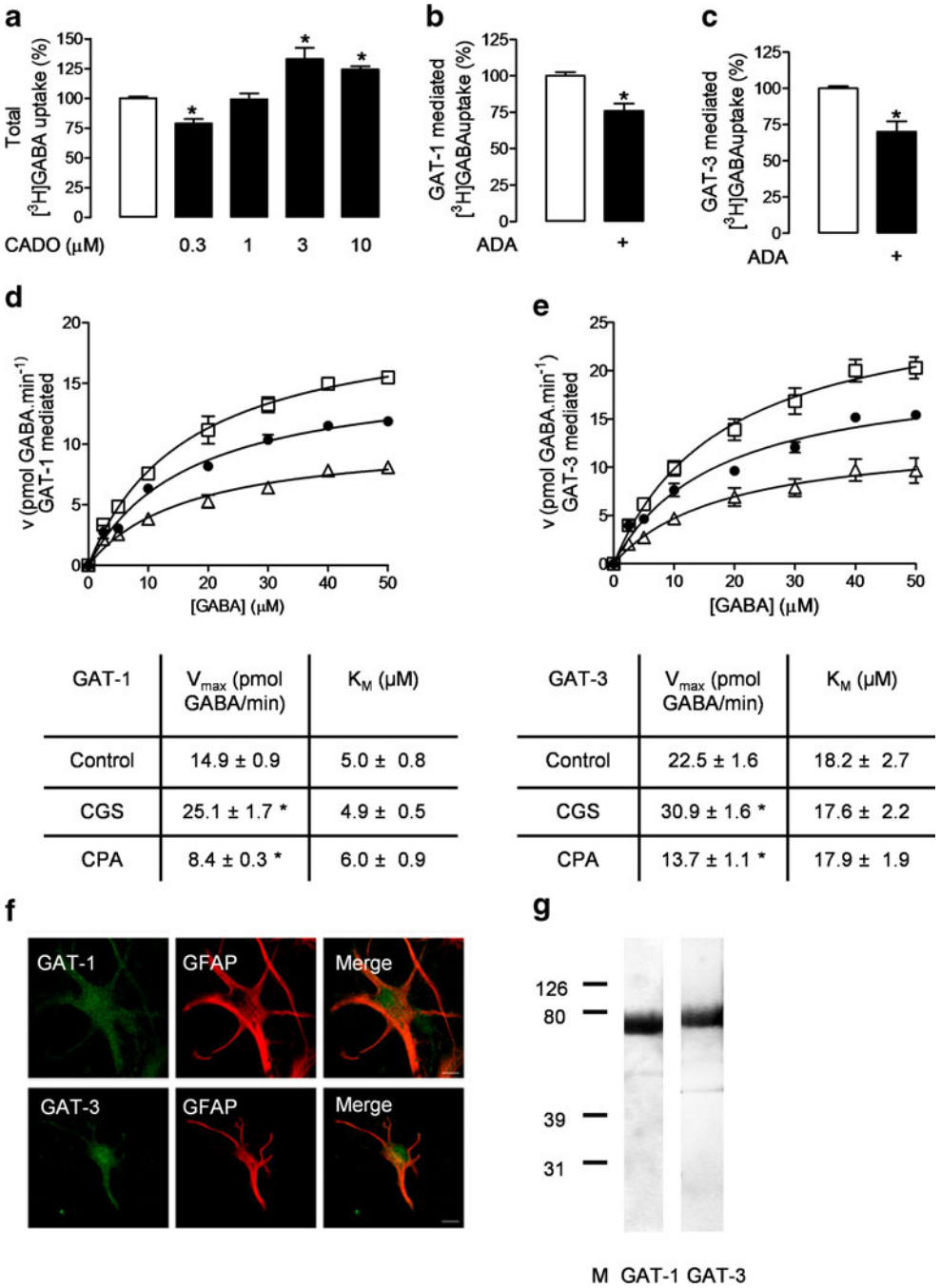

GAT-1	V_{max} (pmol GABA/min)	K_M (μM)
Control	14.9 ± 0.9	5.0 ± 0.8
CGS	25.1 ± 1.7 *	4.9 ± 0.5
CPA	8.4 ± 0.3 *	6.0 ± 0.9

GAT-3	V_{max} (pmol GABA/min)	K_M (μM)
Control	22.5 ± 1.6	18.2 ± 2.7
CGS	30.9 ± 1.6 *	17.6 ± 2.2
CPA	13.7 ± 1.1 *	17.9 ± 1.9

Fig. 1 Adenosine receptor activation modulates [^{3}H]GABA uptake in astrocytes. Astrocytes were incubated with medium or with increasing CADO concentrations (**a**) or 1 U/ml of ADA (**b** and **c**) and the total [^{3}H]GABA uptake (**a**) or GAT-1 (**b**) or GAT-3 (**c**) mediated uptake was determined. In **d** and **e**, uptake was determined using increasing [^{3}H]GABA concentrations in the absence (*circles*) or presence of selective adenosine receptor agonists; the $A_{2A}R$ agonist CGS 21680 (30 nM, *squares*) enhanced and the A_1R agonist CPA (30 nM, *triangles*) decreased the maximum velocity of GAT-1 (**d**) or GAT-3 (**e**) mediated uptake with no changes in K_M values; kinetic values for each condition are shown at the bottom of each panel. In **a**, **d**, and **e** astrocytes were pre-incubated with ADA (1 U/ml) before addition of the agonists (see "Material and methods" section). In **f** immunohistochemistry analysis of GAT-1 is illustrated (*green*, *upper row*) and GAT-3 (*green*, *lower row*) expression by astrocytes; GFAP (*red*) was used as astrocyte marker; *scale bar* 10 μm. In **g**, solubilized astrocytes were analyzed by SDS-PAGE and immunoblotted using rabbit anti-GAT-1 antibody (1:100) or rabbit anti-GAT-3 antibody (1:200) (*M* molecular mass markers). Results in **a**–**e** are shown as mean ± SEM of four to six independent experiments. Statistical significance was calculated by one-way ANOVA followed by Bonferroni multiple comparison test (**a**, **d**, and **e**) or by the Mann–Whitney nonparametric test (**b** and **c**); *$p<0.05$ vs control

voltage to the measured current for each well is the impedance. The data shown refer to the maximum complex impedance induced extracellular currents (dZiec) response to the ligand addition.

Drugs

ADA (E.C. 3.5.4.4, 200 U/mg in 50 % glycerol (*v*/*v*), 10 mM potassium phosphate) was acquired from Roche. GABA (γ-aminobutyric acid) was obtained from Sigma and the [^{3}H] GABA (4-amino-n-[2, 3-^{3}H]butyric acid) specific activity 87.00 Ci/mmol and [^{35}S]GTPγS specific activity 1250 Ci/mmol were obtained from PerkinElmer (Boston, MA, USA). [^{3}H]R–PIA (30.5 Ci/mmol) was from Moravek Biochemicals (Brea, CA, USA). CGS 21680 (4-[2-[[6-amino-9-(*N*-ethyl-β-D-ribofuranuronamidosyl)-9H-purin-yl]amino]ethyl]benzenepropanoic acid hydrochloride), SCH 58261 (2-(2-furanyl)-7-(2-phenylethyl)-7H-pyrazolo[4,3-e][1,2,4]triazolo[1,5-c]pyrimidin-5-amine), CPA (N^6-cyclopentyladenosine), DPCPX (8-cyclopentyl-1,3-dipropylxanthine), SKF 89976A hydrochloride (1-(4,4-diphenyl-3-butenyl)-3-piperidinecarboxylic acid hydrochloride), SNAP 5114 (1-[2-[*tris*(4-methoxyphenyl)methoxy] ethyl]-(S)-3-piperidinecarboxylic acid) and U73122 (1-[6-[[(17β)-3-methoxyestra-1,3,5(10)-trien-17-yl]amino]hexyl]-1*H*-pyrrole-2,5-dione) were obtained from Tocris. 2-Chloroadenosine (CADO), PTx and ChTx, forskolin, Rp-cyclic 3′,5′-hydrogen phosphorothioate adenosine triethylammonium salt (Rp-cAMPs), and R-PIA were obtained from Sigma.

Statistical analysis

From the indicated number of experiments/replicates, data are given as mean ± SEM. To test for statistical significance, the data were analyzed by one-way ANOVA followed by Bonferronni correction for multiple comparisons or by Mann–Whitney nonparametric test (when only two means are analyzed). Values of $p<0.05$ were considered to represent statistically significance.

Results

Endogenous adenosine tonically modulates GABA uptake

To assess the role of adenosine upon GABA uptake, we first incubated the astrocytes with different concentrations of CADO, an adenosine analog with similar affinity for A_1R and A_2R that is resistant to hydrolysis or uptake by the cells, and in conditions where endogenous adenosine had been removed by pre-incubating the astrocytes with adenosine deaminase (ADA, 1 U/ml, see "Material and methods" section). At a relatively low CADO concentration (0.3 μM), there was an inhibition of total GABA taken up by astrocytes, while at higher concentrations (3–10 μM) CADO facilitated total GABA uptake (Fig. 1a). This biphasic influence on GABA transport could either be due to activation of different adenosine receptors, namely A_1R and A_{2A}R, or to a differential influence over the two GATs present in astrocytes, GAT-1 and GAT-3 (Fig. 1f–g). Hence, GAT-1 or GAT-3 activity was independently assayed (see "Material and methods" section). The removal of endogenous adenosine with ADA (1 U/ml) led to a decrease in GABA transport and this decrease was significant either when transport was mediated by GAT-1 (Fig. 1b) or by GAT-3 (Fig. 1c), suggesting that under the present experimental conditions extracellular adenosine was tonically facilitating GAT-1 and GAT-3 activity. When endogenous adenosine had not been removed by pre-incubation with ADA, CADO at a low concentration (1 μM) already enhanced GABA transport (33±9 %, $n=3$, $p<0.05$), most probably because the effect of endogenous and the exogenous agonists is additive; at a higher concentration (10 μM) CADO caused a pronounced decrease in GABA transport (46±3 %, $n=3$, $p<0.05$), compatible with receptor internalization due to receptor overstimulation (see below). To control occupation of adenosine receptors with known agonist concentrations and to avoid variability due to differences in endogenous adenosine in different cultures [see also 20], all subsequent transport assays

Table 1 Binding affinity of agonists and antagonists of adenosine receptors (Ki values in nM with 95 % confidence intervals or ± SEM in parentheses), adapted from [8].

Drug	A_1R	A_{2A}R	A_{2B}R	A_3R
CPA	2.3 (1.5–3.4)[a]	790 (470–1,360)[a]	34,400 (±11,100)[b] 21,000 (±4,300)[d]	43 (30–61)[a]
CGS 21680	290 (230–360)[a]	27 (12–59)[a]	361,000 (±21,100)[b]	67 (50–90)[a]
DPCPX	3.9 (3.5–4.2)[a]	129 (35–260)[a]	50 (±3.7)[b] 51 (±6.1)[d]	4,000 (2,600–6,000)[a]
SCH 58261	290 (210–410)[c]	0.6 (0.5–0.7)[c]		>10,000[c]

[a] [40]
[b] [41]
[c] [42]
[d] [43]

were performed in cells pre-incubated with ADA (1 U/ml; see "Material and methods" section).

A_1R activation decreased and $A_{2A}R$ activation enhanced GABA uptake

Selective agonists of A_1R and $A_{2A}R$ were used to clarify the influence of the adenosine receptors upon GABA transporters. The selective A_1R agonist, CPA (30 nM), decreased maximal velocity (V_{max}) of GABA transport mediated by GAT-1 (Fig. 1d) or by GAT-3 (Fig. 1e), whereas the selective agonist for $A_{2A}R$, CGS 21680 (30 nM) enhanced V_{max} for GAT-1 (Fig. 1d), and for GAT-3 (Fig. 1e), without affecting transport (K_M) values ($p>0.05$, $n=6$). These data indicate that adenosine receptor activation modified maximum transport capacity rather than in the affinity of the transporters for GABA, and that inhibition of GAT-1 and GAT-3 is mediated by A_1R, whereas facilitation requires $A_{2A}R$ activation. To further confirm that A_1R and $A_{2A}R$ affect GABA transport in opposite ways, we used combinations of agonists and antagonists selective for either receptor (see Table 1). Results are summarized in Fig. 2. CPA and CGS 21680 effect were measured in

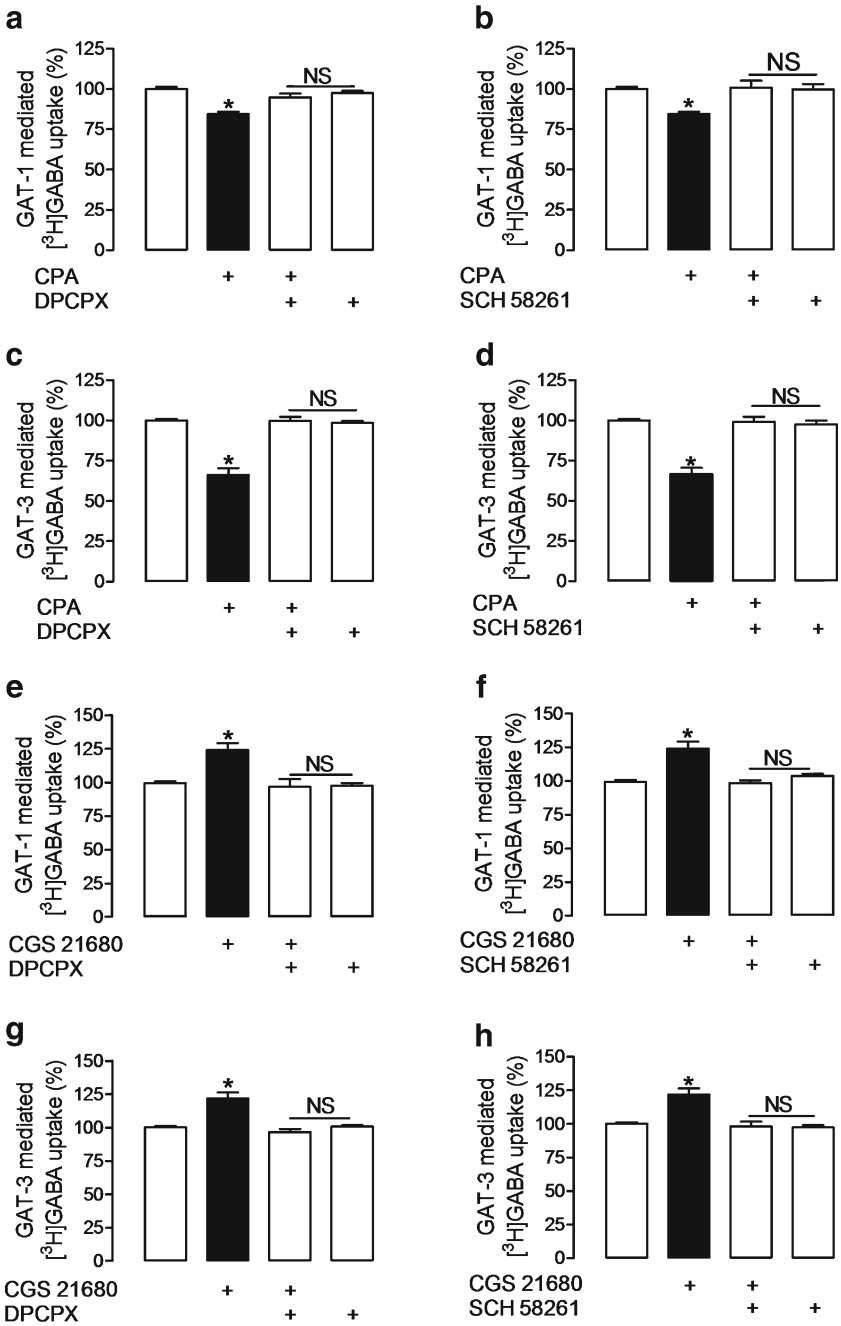

Fig. 2 Inhibition of [^{3}H]GABA uptake is mediated by A_1R, while facilitation is mediated by $A_{2A}R$. Astrocytes were treated for 15 min with 1 U/ml ADA (see "Material and methods" section) before the addition of medium, the A_1R antagonist DPCPX (50 nM) or the $A_{2A}R$ antagonist SCH 58261 (50 nM). After 20 min, the A_1R agonist CPA (30 nM; **a**–**d**) or the $A_{2A}R$ agonist CGS 21680 (30 nM; **e**–**h**) were added and GAT-1 (**a**, **b**, **e**, **f**), or GAT-3 (**c**, **d**, **g**, **h**) mediated [^{3}H]GABA uptake was measured as indicated in "Material and methods" section. Results are mean ± SEM of six independent experiments. Statistical significance was calculated by one-way ANOVA followed by Bonferroni multiple comparison test; *$p<0.001$ compared with control (*left bar*); NS, $p>0.05$

the presence of the A_1R-selective antagonist, DPCPX (50 nM) or the $A_{2A}R$ selective antagonist, SCH 58261 (50 nM). Surprisingly, the effect of the A_1R agonist was fully prevented not only by previous blockade of the A_1R with DPCPX but also by the blockade of $A_{2A}R$ with SCH 58261. For these experiments, the concentration of each compound was chosen to act in a selective way. Analogously, facilitation of GABA transport by the $A_{2A}R$ agonist, CGS 21680, was completely abolished by the blockade of either $A_{2A}R$ or A_1R. These results strongly indicate that A_1R and $A_{2A}R$ are tightly interacting and represent a clear example of cross-antagonism between the two receptors. Such antagonism may be due to heteromerization [21, 22] thus we decided to test whether A_1R and $A_{2A}R$ may form heteromers in astrocytes.

A_1R–$A_{2A}R$ heteromers in astrocytes

The BRET approach was used to evaluate the ability of A_1R to heteromerize with $A_{2A}R$ in astrocytes. First, the endogenous A_1R and $A_{2A}R$ expression in astrocytes was investigated by Western blot (Fig. 3a and b). A_1R and $A_{2A}R$ expression is relatively low at 2 weeks of cell culture but increases later on. Thus, to avoid competition with endogenous receptors, BRET measurements were performed using 2-week cultured astrocytes transiently co-transfected with a constant amount of $A_{2A}R$–RLuc (7.5 μg cDNA) and increasing amounts of A_1R–YFP (4–15 μg cDNA). Fusion of RLuc to $A_{2\ A}R$ or to YFP to A_1R did not modify receptor function as determined by cAMP assays [16 and results not shown]. A positive and saturable BRET signal was found for the pair $A_{2A}R$–RLuc and A_1R–YFP (Fig. 3c). From the saturation curve, a $BRET_{max}$ of 94±15 mBU and a $BRET_{50}$ of 16±2 were calculated. As a negative control, the $A_{2A}R$–RLuc and serotonin $5HT_{2B}R$–YFP pair was used. As shown in Fig. 3c, the negative control gave a linear nonspecific BRET signal, thus confirming the specificity of the interaction between $A_{2A}R$–RLuc and A_1R–YFP in astrocyte primary cultures.

Ligand binding assays to receptor heteromers in isolated membranes usually reveal a "biochemical fingerprint" which consists of changes in ligand binding characteristics of one receptor when the partner receptor is occupied by agonist [23]. No intracellular cross-talk can occur in extensively washed disrupted membranes and therefore it can be assumed that the "fingerprint" results from intramembrane receptor–receptor direct or indirect interactions. Although an indirect approach, it is accepted as identifier of receptor heteromers in native tissues or in cells expressing the natural nonheterologous receptors [23]. Therefore, binding experiments were performed to identify native A_1R–$A_{2A}R$ heteromers in 4-week cultured astrocytes. As shown in Fig. 3d, the displacement of A_1R agonist [^{3}H]R–PIA binding by the $A_{2A}R$ agonist, CGS 21680 (but not by the $A_{2A}R$ antagonist, SCH 58261) was significantly ($p<0.01$) better represented by a biphasic than by a monophasic curve. It is not expected that the $A_{2A}R$ agonist, at concentrations lower than 500 nM, would significantly bind to A_1R (<1 % binding to A_1R, according to known K_D value). However, 500 nM CGS 21680 significantly ($p<0.05$) displaced the binding of the selective A_1R agonist, [^{3}H]R–PIA, with an IC_{50} value of 90±30 nM. Obviously, higher concentrations of CGS 21680 caused a further displacement of [^{3}H]R–PIA binding that, according to its IC_{50} value (8±4 μM), reflects the binding of CGS 21680 to the A_1R. As expected, the $A_{2A}R$ antagonist, SCH 58261, only displaced A_1R agonist binding (IC_{50} of 500±120 nM) at concentrations known to lose $A_{2A}R$ selectivity and to bind to A_1R (Fig. 3d). Taken together, these data indicate that the biphasic [^{3}H]R–PIA binding displacement curve observed in the presence of the $A_{2A}R$ agonist constitutes a fingerprint of the A_1R–$A_{2A}R$ heteromer in nontransfected primary cultured astrocytes.

To evaluate whether A_1R–$A_{2A}R$ heteromerization could be influenced by agonist or antagonist binding, a series of experiments was performed in transiently co-transfected HEK-293T cells using a constant amount of $A_{2A}R$–RLuc (1.5 μg cDNA) and increasing amounts of A_1R–YFP (1–8 μg cDNA). In agreement with previous results [13], a positive and saturable BRET signal was found. Stimulation (20 min) with the $A_{2A}R$ agonist (CGS 21680, 30 nM; Fig. 3e), or with the A_1R agonist (CPA, 30 nM; Fig. 3f) did not promote any consistent ($p>0.05$) change in $BRET_{max}$ or $BRET_{50}$ values. Similar BRET values were also obtained in the presence or absence of $A_{2A}R$ (Fig. 3g) or A_1R (Fig. 3h) antagonists indicating that neither agonist nor antagonist binding affected the receptor oligomerization state.

Fig. 3 A_1R–$A_{2A}R$ heteromers in astrocytes. In **a**, the expression of A_1R and $A_{2A}R$ in astrocytes after different weeks of culture was detected by western blot as indicated in methods using alfa-tubulin as loading control. Averaged densitometric analysis of immunoblots is shown in **b**; data are mean ± SEM of three to four determinations; statistical significance was calculated by the Mann–Whitney nonparametric test; *$p<0.05$ compared with 2 weeks of culture. In **c**, **e**, **f**, **g**, and **h** BRET saturation experiments were performed using 2 weeks cultured astrocytes (**c**) or HEK-293 cells (**e**–**h**) co-transfected with 1.5 μg (**c**) or 1 μg (**e**–**h**) cDNA corresponding to $A_{2A}R$-Rluc and increasing amounts of cDNA corresponding to A_1R–YFP (*squares*) or $5HT_{2B}$-YFP (*triangles*, as negative control) constructs; 2 weeks cultured astrocytes were used to minimize competition between the transfected and native receptors. In (**e**–**h**) cells were treated for 10 min with medium (*squares*, *solid line*) or with 30 nM CGS 21680 (**e**), 30 nM CPA (**f**), 50 nM SCH 58261 (**g**) or 50 nM DPCPX (**h**) (*circles*, *dotted lines*). The $BRET_{max}$ and $BRET_{50}$ values are shown in the *inserts*. Both fluorescence and luminescence of each sample were measured before every experiment to confirm similar donor expressions (about 100,000 luminescent units) while monitoring the increase acceptor expression (500–10,000 fluorescent units). Data are means ± SEM of three different experiments grouped as a function of the amount of BRET acceptor. In **d** competition experiments of 0.8 nM [^{3}H]R–PIA versus increasing concentrations of the A_{2A} receptor agonist, CGS 21680 (*solid line*), or the A_{2A} receptor antagonist, SCH 58261 (*dotted line*), were performed using astrocytic membranes (0.18 mg protein/ml). Data are mean ± SEM of a representative experiment ($n=3$) performed in triplicates

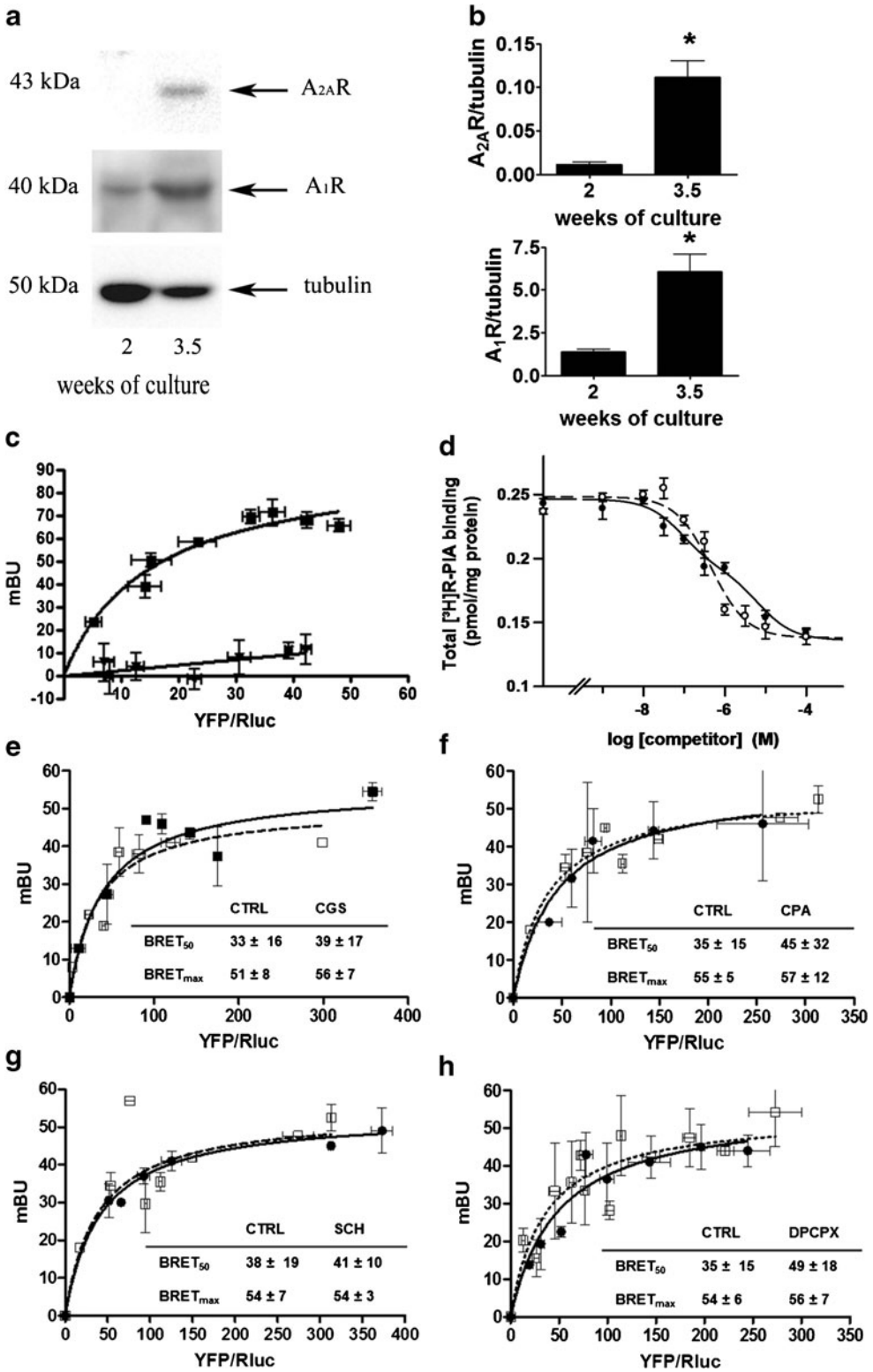

A_1R or $A_{2A}R$ activation, but not its blockade, leads to internalization of the heteromers

Heteromerized receptors are expected to internalize together. To test this possibility, agonist-mediated internalization of A_1R and $A_{2A}R$ was studied in astrocytes. Western blot data clearly showed that A_1R immunoreactivity at the cell surface did not only decrease after incubation of astrocytes with the A_1R agonist, but also after incubation with the $A_{2A}R$ agonist (Fig. 4a). This decrease was accompanied by an increase in

A_1R immunoreactivity in the intracellular fraction (Fig. 4b). No significant changes in surface (Fig. 4c) or intracellular (Fig. 4d) A_1R immunoreactivity were detected upon incubation with either A_1R or A_2R antagonists, suggesting that, under the experimental conditions used, endogenous extracellular adenosine was not tonically inducing receptor recycling, and that receptor internalization might require receptor overstimulation (Fig. 4a, b). Interestingly, when the A_1R agonist was added after previous blockade of either A_1R or $A_{2A}R$ by the selective antagonists, it was no longer able to modify A_1R immunoreactivity at the cell surface (Fig. 4e) or in the intracellular fraction (Fig. 4f). Similarly, adding the $A_{2A}R$ agonist after a previous blockade of A_1R or $A_{2A}R$ did not promote any modification of A_1R immunoreactivity at cell surface (Fig. 4e) or in the intracellular fraction (Fig. 4f). It therefore becomes clear that blockade of either A_1R or $A_{2A}R$ prevents A_1R internalization induced by exposure to A_1R or $A_{2A}R$ agonists.

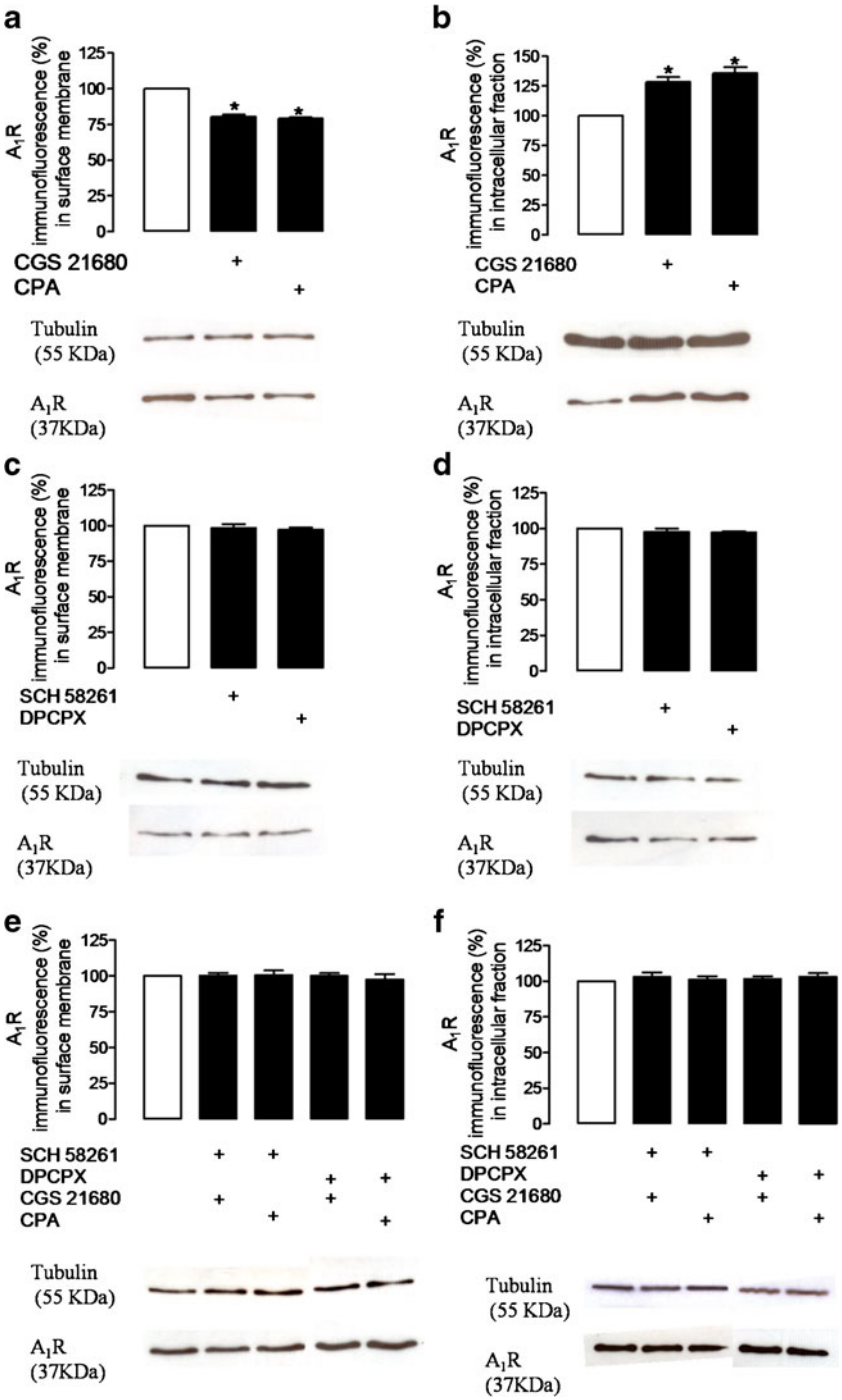

Fig. 4 A_1R or $A_{2A}R$ activation (but not its blockade) in astrocytes promotes internalization of A_1R. Astrocytes were incubated in the absence of ADA, for 30 min with the A_1R agonist CPA (30 nM) or with the $A_{2A}R$ agonist CGS 21680 (30 nM), alone (**a** and **b**) or in the presence of either the A_1R antagonist DPCPX (50 nM) or the $A_{2A}R$ antagonist SCH 58261 (50 nM) (**e** and **f**), or only with DPCPX (50 nM) or SCH 58261 (50 nM) (**c** and **d**), before starting the biotinylation protocol. When testing the action of agonists in the presence of antagonists, the antagonists were added 15 min before the agonists. A_1R expression at surface membranes (*left*) and intracellular fraction (*right*) was determined as indicated in "Material and methods" section. Data illustrated in panels **e** and **f** were obtained, in each experiment, from two gels due to sample number limitations (maximum, four per gel) of the required system (high-volume sample loading); gels from the same experiment were processed and immunoblotted together under the same conditions. Results are mean ± SEM of five independent experiments. Statistical significance was calculated by one-way ANOVA followed by Bonferroni multiple comparison test; *$p<0.001$ compared with control (100 %, *white bar*)

Co-internalization of A_1R and $A_{2A}R$ after incubation with A_1R or $A_{2A}R$ agonists was also assessed by confocal microscopy analysis of HEK-293T cells co-expressing A_1R–YFP and $A_{2A}R$–RLuc. After exposure to either A_1R- or $A_{2A}R$-selective agonists, intracellular A_1R–YFP fluorescence and $A_{2A}R$–RLuc immunoreactivity markedly increased; a similar phenomenon was observed after exposure to an A_1R agonist but not after exposure to A_1R or $A_{2A}R$ antagonists (Fig. 5). Collectively, these results indicate that A_1R and $A_{2A}R$ do internalize together in response to A_1R- or $A_{2A}R$-selective agonist binding.

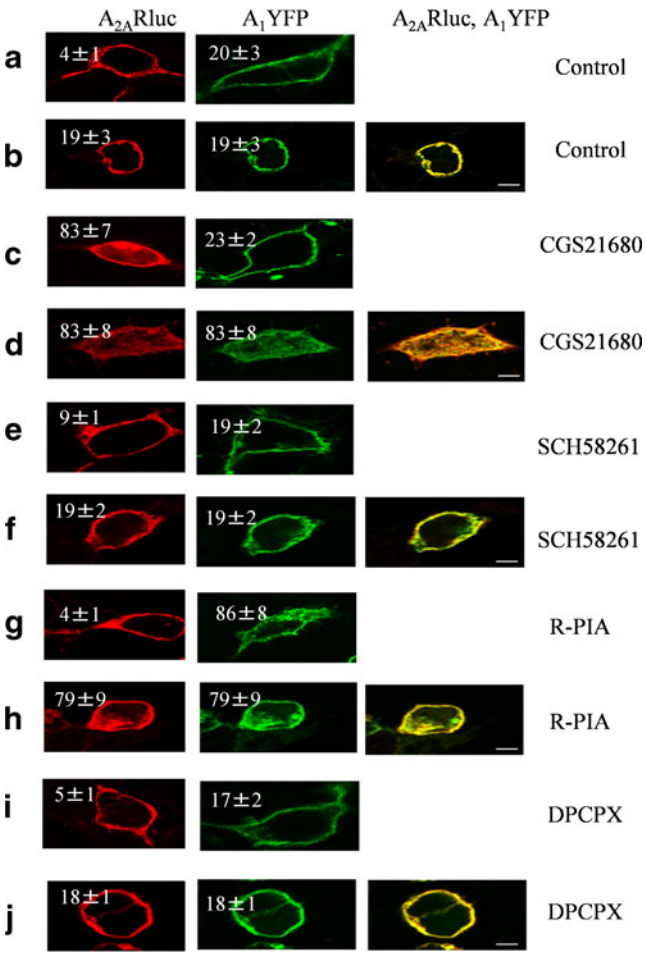

Fig. 5 A_1R and $A_{2A}R$ are internalized together upon exposure to either A_1R or $A_{2A}R$ agonists. HEK-293 cells were transfected with 1 μg cDNA corresponding to $A_{2A}R$-Rluc (*red*) or 1 μg cDNA corresponding to A_1R–YFP (*green*) (**a**, **c**, **e**, **g**, **i**) or both (**b**, **d**, **f**, **h**, **j**) and 48 h post-tranfection cells were treated for 60 min with medium (**a** and **b**), 100 nM $A_{2A}R$ agonist CGS 21680 (**c** and **d**), 1 μM A2AR antagonist SCH 58261 (**e** and **f**), 100 nM A_1R agonist R-PIA (**g** and **h**) or 1 μM A_1R antagonist DPCPX (**i** and **j**). Immunocytochemistry was performed as indicated in "Material and methods" section and $A_{2A}R$–RLuc was labeled with the anti-RLuc antibody and A_1R–YFP was detected by its fluorescence properties. Colocalization is shown in *yellow*. The quantification of receptor internalization after the exposure to ligands was determined by analyzing, for each condition, 40–50 cells from 12 different fields in three independent preparations by confocal microscopy. *Scale bar* 5 μm and it applies to all panels. Values are expressed as mean ± SEM

The A_1R–$A_{2A}R$ heteromer is coupled to $G_{i/0}$ and G_s proteins

To figure out which G protein(s) is (are) coupled to the A_1R-A_AR heteromer, [^{35}S] GTP-γ-S binding assays followed by immuno-precipitation using antibodies against different G proteins (G_s, $G_{i/0}$, and $G_{q/11}$) were performed. The approach is similar to that reported by Rashid and colleagues to identify $G_{q/11}$ coupling to the dopamine D_1–D_2 receptor heteromer [24]. As illustrated in Fig. 6a (left panel), the A_1R-selective agonist (CPA, 30 nM) but not the $A_{2A}R$-selective agonist CGS 21680 (30 nM) significantly increased the $G_{i/0}$ activity, an effect unpredictably prevented by the $A_{2A}R$ selective antagonist. In what concerns G_s activity (Fig. 6a, middle panel), it was enhanced by the $A_{2A}R$ selective agonist CGS 21680 (30 nM), but not by the A_1R agonist, CPA (30 nM); again, and unpredictably, the effect of the $A_{2A}R$ agonist was fully abolished by the A_1R antagonist, DPCPX (50 nM). None of the adenosine receptor agonists affected $G_{q/11}$ activity, which was enhanced by acetylcholine (10 μM), used as a positive control in the same batch of astrocytic membranes (Fig. 6c, right panel). These data suggest that A_1R–A_2R heteromers are coupled to both $G_{i/0}$ and G_s proteins and not to a unique $G_{q/11}$ protein.

G protein activity may be permanently modified by the binding of several toxins, thus these are useful tools to dissect out a differential receptor-G protein coupling in intact cells and to evaluate the functional consequences of G-protein-mediated-signaling blockade. GABA uptake assays were therefore performed using ChTx, which uncouples G_s from the receptors due to ADP-ribosylation and permanent activation of the α_S-subunit [25], as well as using PTx, which catalyzes the ADP-ribosylation of the α $G_{i/0}$ subunit and locks it in the GDP-bound inactive state thus preventing $G_{i/0}$ protein activation [26]. Inhibition of either GAT-1- or GAT-3-mediated GABA uptake induced by the A_1R agonist, CPA, was fully prevented by PTx, but, interestingly, this toxin also prevented $A_{2A}R$-mediated facilitation of GAT-1- and GAT-3-mediated GABA uptake (Fig. 6b). Similar results were obtained in the reciprocal experiment using ChTx. In fact, the toxin prevented not only the facilitation of GAT-1- and GAT-3-mediated transport caused by the $A_{2A}R$ agonist, CGS 21680, but also the inhibition of GABA transport mediated by the A_1R agonist, CPA (Fig. 6c). The ChTx and PTx data strongly suggest that the A_1R–$A_{2A}R$ heteromer is coupled to both G_s and $G_{i/0}$ proteins. The results also indicate that if one G protein (G_s or $G_{i/0}$) is blocked or receptor-uncoupled, both A_1R and $A_{2A}R$ agonists lose their effect upon GABA uptake. It seems that the A_1R–$A_{2A}R$ heteromer is the mediator of both the inhibitory and the excitatory effects triggered by, respectively, CPA and CGS 21680.

As a further approach, $G_{i/0}$, G_S, or $G_{q/11}$ activity was also measured by the CellKey label-free assay (see "Material and methods") in intact CHO cells transfected either with A_1R,

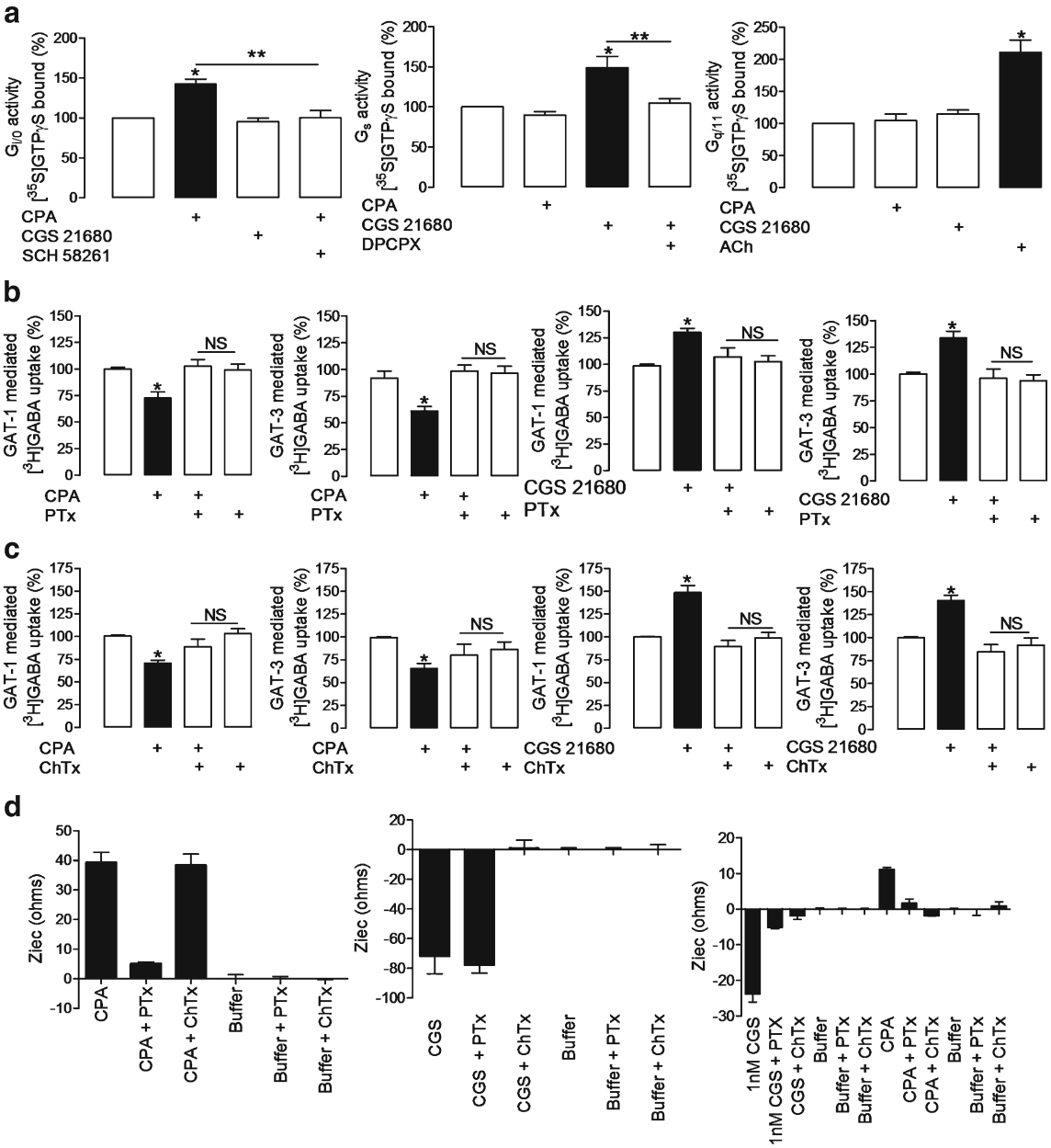

Fig. 6 A_1R–$A_{2A}R$ heteromer in astrocytes is coupled to both G_s and $G_{i/0}$. In **a** GTP-γ-[^{35}S] assays were performed as described in "Material and methods" section to test $G_{i/0}$ activity (*left*), G_s activity (*middle*), or $G_{q/11}$ activity (*right*) using membranes from astrocytes treated for 10 min with medium, the $A_{2A}R$ antagonist SCH 58261 (50 nM) or the A_1R antagonist DPCPX (50 nM) prior the activation with $A_{2A}R$ agonist CGS 21680 (30 nM) or A_1R agonist CPA (30 nM) or Ach (10 μM) as positive control. In **b** and **c**, astrocytes were treated with medium, PTx (**b**, 5 μg/ml) or ChTx (**c**, 5 μg/ml) prior to stimulation with CPA (30 nM) or CGS 21680 (30 nM) and GAT-1 and GAT-3 mediated [^{3}H]GABA uptake was measured as indicated in "Material and methods" section. Toxins were pre-incubated with the astrocytes for 4 h and then removed prior to uptake assays. **d** CellKey label-free assays were performed in CHO cells stable expressing A_1R (*left*), $A_{2A}R$ (*middle*), or both (*right*), treated with medium, PTx (10 ng/ml) or ChTx (100 ng/ml) and stimulated or not with CGS 21680 (10 nM) or CPA (10 nM). Results are as mean ± SEM from four to eight independent experiments. Statistical significance was calculated by one-way ANOVA followed by Bonferroni multiple comparison test; *$p<0.001$ compared with control (100 %, *left bar* in **a**–**c**), **$p<0.001$ compared with cells treated with the agonist in the absence of the antagonist. NS, $p>0.05$

$A_{2A}R$ or both. In A_1R-transfected cells, the signaling obtained upon A_1R activation with the agonist CPA (10 nM) showed a $G_{i/0}$ profile (increases in impedance) that was completely blocked when cells were treated with PTx. Impedance did not significantly change when cells were treated with ChTx (Fig. 6d, left panel). In $A_{2A}R$ transfected cells, the $A_{2A}R$ agonist CGS 21680 (10 nM) induced a G_s profile (decreases in impedance) that was completely blocked when cells were treated with ChTx but not significantly modified upon PTx treatment (Fig. 6d, middle panel). Interestingly, in cells co-

expressing $A_{2A}R$ and A_1R the impedance profiles obtained by activation with CPA ($G_{i/0}$ profile) or CGS 21680 (G_s profile) were fully blocked by either PTx or ChTx (Fig. 6d, right panel). These results strongly reinforce the notion that the A_1R–$A_{2A}R$ heteromer is coupled to both G_s and $G_{i/0}$ proteins.

A transducing unit constituted by an A_1R–$A_{2A}R$ heteromer

The above-described data strongly supports the notion that the heteromer is coupled to $G_{i/0}$ and G_S and not to $G_{q/11}$. This arrangement predicts that the transducing system operated by adenosine receptors to modulate GABA transport into astrocytes is centered in the adenylate cyclase/cAMP/PKA cascade. To address the question of whether a single cAMP/PKA-centered transducing unit is able to both inhibit and facilitate GABA transport, we tested the influence of drugs known to interfere with this transducing pathway upon the effect of A_1R and $A_{2A}R$ receptor agonists on GABA transport. In addition, we also tested the blocker of phospholipase C (PLC), in order to evaluate a putative transducing pathway classically associated to $G_{q/11}$.

The inhibitory action of A_1R agonist upon GAT-1 (Fig. 7a) and GAT-3 (Fig. 7c) still occurred in the presence of PLC blocker U73122 (3 μM) [27], but it was totally abolished by the blockade of PKA by Rp-cAMPs (100 μM) [28]. The activation of adenylate cyclase with a supramaximal concentration of forskolin (10 μM) [29], per se, increased GABA transport and occluded the inhibitory effect of the A_1R agonist (CPA) upon GABA transport (Fig. 7a, c). The facilitatory effect of the $A_{2A}R$ agonist, CGS 21680, was not affected by the PLC inhibitor, U73122, but was totally impaired by the PKA blocker, Rp-cAMPs. The adenylate cyclase activator, forskolin, mimicked the action of the $A_{2A}R$ agonist and its facilitatory effect was not additive with that of CGS 21680, indicating a common mechanism (Fig. 7b, d).

Discussion

The work now reported clearly shows that GABA uptake by astrocytes is under modulation by extracellular adenosine, which, by interacting with a functional unit constituted by A_1R–$A_{2A}R$ heteromers coupled to two distinct G proteins, $G_{i/0}$ and G_s, can either boost or depress the amount of inhibitory neurotransmitter available to neurons.

Using an adenosine analog, CADO, with high structural similarity to adenosine but with the advantage of not being taken up by the cells nor metabolized by ecto-enzymes, and after clearing up endogenous adenosine, we observed that submicromolar concentrations of the stable agonist inhibit GABA uptake while at low micromolar concentrations there is an enhancement of GABA transport. Considering that the affinity of adenosine for the A_1R is slightly higher than for the $A_{2A}R$ [8], it is likely that the inhibition was mediated by A_1R and facilitated by $A_{2A}R$. Accordingly, the A_1R selective agonist, CPA, inhibited GABA uptake into astrocytes, while the $A_{2A}R$ selective agonist, CGS 21680 facilitated it. Unexpectedly, the blockade of either receptor with selective antagonists prevented the effects mediated by either agonist, a strong indication that A_1R and $A_{2A}R$ are interacting at the molecular level in primary cortical astrocytes. Abundant evidence of A_1R–$A_{2A}R$ functional crosstalk has been described, namely, $A_{2A}R$ activation attenuates A_1R-mediated responses in the hippocampus [10, 11], at the neuromuscular junction [9], and in transfected cells [13]; however, no attempt has been made to unequivocally and directly identify A_1R–$A_{2A}R$ heteromerization in neural cells. Thus, we looked for energy transfer in primary cultures of astrocytes transfected with cDNAs for $A_{2A}R$–RLuc and A_1R–YFP. In these assays, a positive, specific, and saturable BRET signal for the energy transference between $A_{2A}R$–RLuc and A_1R–YFP was detected in living primary astrocytes. Moreover, the heteromer in native astrocytes was detected by looking for a "fingerprint" which consists of changes in ligand binding characteristics of A_1R when the $A_{2A}R$ is activated. These results complemented and strengthened the evidence for A_1R–$A_{2A}R$ heteromerization in nontransfected astrocytes. Evidence for A_1R–$A_{2A}R$ heteromers in living tissues awaits further development of the already-available BRET–FRET near-infrared dot technology for in vivo imaging [30], not yet developed for nervous system analysis.

As it is the case for GABA transporters in astrocytes [20], membrane proteins usually recycle, being internalized and sent back to the membrane in a controlled way. Biotinylation assays showed that exposure to either A_1R or $A_{2A}R$ agonists led to decreases in surface expression of A_1R, and to similar increases in the A_1R levels in intracellular fractions. It then appears that binding of a single ligand to the heteromer, either A_1R or $A_{2A}R$, is sufficient to promote internalization. The previous blockade of A_1R or $A_{2A}R$ prevents the internalization mediated by both A_1R and $A_{2A}R$ agonists, suggesting that internalization of heteromer in response to agonists is a consequence of heteromer overactivity. Confocal imaging of transfected HEK-293T cells confirmed that exposure to an A_1R agonist led to internalization of not only A_1R but also $A_{2A}R$ and, conversely, exposure to an $A_{2A}R$ agonist led to internalization of not only $A_{2A}R$ but also A_1R. Thus, in this aspect, A_1–$A_{2A}R$ heteromers behaved as the β2-adrenoceptor-δ-opioid [31] and μ-opioid-tachykinin NK1 [32] receptor heteromers but different from other heteromers whose protomers do not co-internalize [see 33]. It is technically difficult to know to what extent adenosine receptor internalization affects GABA transport in astrocytes. In fact, GABA transport into astrocytes is itself affected by inhibitors of arrestin-dependent endocytosis [20] that would be required to prevent adenosine receptor internalization.

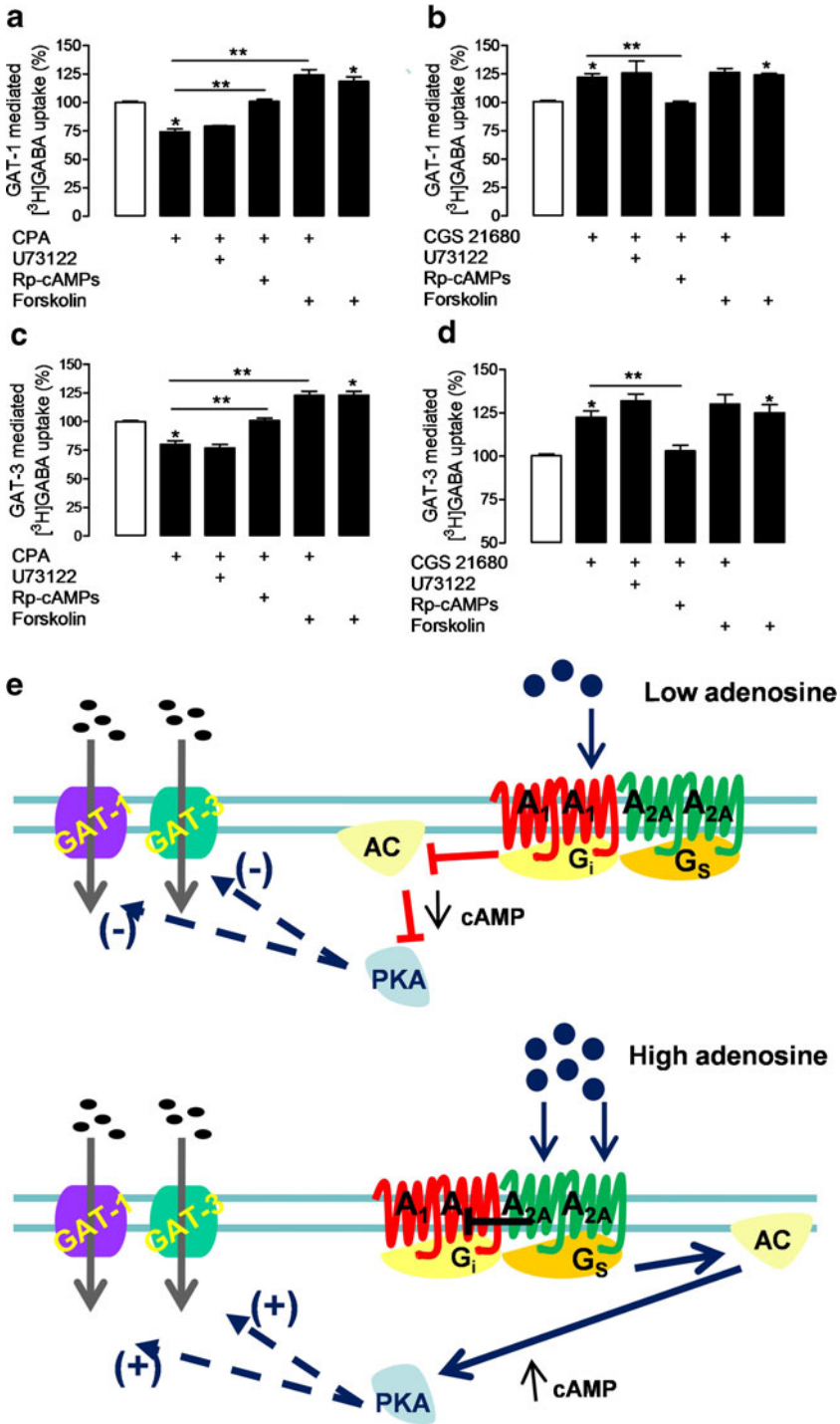

Fig. 7 A_1R–$A_{2A}R$ heteromer signaling. Astrocytes were treated for 15 min with 1 U/ml ADA (see "Material and methods" section) before the addition of medium, the PLC inhibitor U73122 (3 μM), the PKA inhibitor Rp-cAMPs (100 μM) or the adenylate cyclase enhancer forskolin (10 μM). After 20 min, the A_1R agonist CPA (30 nM) (**a** and **c**) or the $A_{2A}R$ agonist CGS 21680 (30 nM) (**b** and **d**) were added and the GAT-1 (**a** and **b**) or GAT-3 (**c** and **d**) mediated [^{3}H]GABA uptake was measured as indicated in Methods. Results are mean ± SEM from four to ten independent experiments. Statistical significance was calculated by one-way ANOVA followed by Bonferroni multiple comparison test; *p<0.001 vs control (100 %, *left bars*), **p<0.001 vs cells treated with the agonist alone. **e** Schematic representation of A_1R–$A_{2A}R$ heteromer function. At low levels, adenosine binds preferentially to the A_1R protomer of the heteromer, which will activate $G_{i/0}$ protein, and through a mechanism that involves adenylate cyclase (AC), and PKA activity, leads to a decrease (*minus sign*) in GABA uptake mediated by GAT-1 and GAT-3. At higher concentrations, adenosine activates the $A_{2A}R$ protomer of the heteromer inhibiting A_1R and, through G_s protein, couples to the AC/cAMP/PKA pathway, leading an enhancement (*plus sign*) of GABA uptake

Agonist exposure did not affect BRET, suggesting that agonist binding does not induce pronounced allosteric modifications in the receptors. It therefore appears that the A_1R–$A_{2A}R$ heteromer in astrocytes mostly works as an integral entity, leaving and probably also reaching the cell surface as a heteromeric structure. Furthermore, since antagonists did not modify the receptor levels at the membrane or the BRET signal, the loss of effect of one agonist upon previous blockade the other receptor cannot be attributed to heteromer disruption or formation. Cross-antagonism, which is considered a heteromer fingerprint [23], is likely due to conformational changes induced by the antagonist and leads to a non-functional state of the signaling receptor by uncoupling it from G-protein-mediated signaling.

Heteromers may couple to G-proteins different from those to which each individual receptor partner usually couple. This is indeed the case of dopamine D_1–D_2 receptor heteromer, which couple to $G_{q/11}$ [24] in a clear shift from the canonical

D_1 coupling to G_s and D_2 coupling to $G_{i/0}$. To identify the transducing system operated by the A_1R–$A_{2A}R$ heteromer in astrocytes, we first used an approach similar to that used by Rashid et al. [24], i.e., [^{35}S] GTP-γ-S binding followed by differential immunoprecipitation. Data obtained allowed to conclude that the A_1R–$A_{2A}R$ heteromer in astrocytes seems to be coupled to both $G_{i/0}$ and G_s proteins. Interestingly, the cross-antagonism was also evident in these assays. Thus, the A_1R agonist, but not the $A_{2A}R$ agonist, increased $G_{i/0}$ activity, but the enhancement was also prevented when the $A_{2A}R$ antagonist was present. Reciprocally, G_s activation, which was restricted to the $A_{2A}R$ agonist, was prevented when the A_1R was blocked with the antagonist. Similar conclusions could be drawn from GABA uptake assays since toxin-induced prevention of coupling of receptors to either G_s or $G_{i/0}$ led to reciprocal impaired function of A_1R or $A_{2A}R$ agonists to modulate GABA transport. The cross-inhibition of heteromer function by the toxins was observed both in cultured astrocytes and in heterologous cells co-expressing A_1R and $A_{2A}R$, but not in cells expressing only one receptor subtype. Altogether, these data provide strong evidence for a heteromeric functional entity regulating GABA uptake by astrocytes. This functional unit consists of an A_1R–$A_{2A}R$ heteromer–$G_{i/0}$–G_s complex, which signals through G_s when the $A_{2A}R$ protomer is activated and through $G_{i/0}$ when the A_1R protomer is activated. Most importantly, the blockade of a single partner in the complex led to adjustments in the whole unit. Since two GPCR molecules cannot bind to more than a single G protein [34], we suggest that A_1R–$A_{2A}R$ heteromers in astrocytes are expressed as heteromers of homomers with a minimal structure consisting of an A_1R-A_1R–$A_{2A}R$-$A_{2A}R$ complex, making possible to accomodate two different G proteins (Fig. 7e). In fact, by BRET with a double luminescence/fluorescence molecular complementation approach, we obtained evidence for the expression of A_1R–$A_{2A}R$ heterotetramers in transfected cells (results sent for publication). The transducing system operated by the heteromer seems to involve the adenylate cyclase, consistent with the G protein data and the data obtained in the presence of forskolin or of the inhibitor of the PKA (Rp-cAMPs), both of which occluded the effects of the A_1R or $A_{2A}R$ selective agonists upon GABA uptake.

A tenfold rise in concentration of the nonselective ligand, CADO, was enough to gate $A_{2A}R$ activation and engage a completely opposite modulation of GABA uptake. Assuming a near tenfold higher potency of CADO as compared to adenosine [35], the shift from inhibition to enhancement of GABA uptake might occur at low micromolar concentrations of extracellular adenosine. These concentrations may be easily attained at a tripartite synapse, where considerable amounts of ATP and adenosine may be released from the astrocytic, the presynaptic or the postsynaptic components [36–38]. The higher the release of purines, as it may occur at high neuronal firing rates in reciprocal neuron-to-astrocyte communication at the tripartite synapse [see 39], the higher the expected concentration of extracellular adenosine. It is therefore likely that sustained neuronal firing promotes activation of the $A_{2A}R$ protomer of the A_1R–$A_{2A}R$ heteromer leading to facilitation of GABA uptake. Activation of GABA uptake by astrocytes would lead to decreased ambient GABA and, consequently, to depression of tonic GABAegic inhibition, and enhancement of the excitatory tonus. Conversely, and according to the concentration–response curve for CADO to modulate GABA transport, at submicromolar adenosine concentrations, a preferential activation of the A_1R protomer of the A_1R–$A_{2A}R$ heteromer might inhibit GABA uptake by astrocytes and enhance tonic inhibition by ambient GABA. Thus, through an adenosine action upon A_1R–$A_{2A}R$ heteromers, astrocytes may behave as dual amplifiers, facilitating excitation at intense astrocytic to neuronal signaling and increasing inhibition at low neuronal firing rates. This switch in neural activity may require a highly efficient control to avoid sudden state transitions, and this is most probably the main advantage of heteromerization of A_1R and $A_{2A}R$ in astrocytes. Indeed, overstimulation of just one of the receptor protomer leads to internalization of the whole functional unit. In what concerns GABA transport, the disappearance of the heteromer would constitute a brake in the system to avoid abrupt inhibitory signaling and/or sudden switch from excitation to inhibition as a consequence of desensitization of only the excitatory protomer.

Conclusions

We herein provide strong and complementary evidence that adenosine has a biphasic effect on GABA uptake, which is mediated by A_1R–$A_{2A}R$ heteromers coupled to both $G_{i/0}$ and G_s proteins. Extracellular adenosine acting on this A_1R–$A_{2A}R$ functional unit may operate in a concerted way to balance a PKA-dependent action on GABA uptake as indicated in the scheme of Fig. 7e. The neural output would most probably be inhibitory at low firing rates and facilitatory at high firing rates. We therefore disclose a so far unknown way through which adenosine by acting on adenosine receptors in astrocytes may significantly contribute to neurotransmission in a dual manner, which depends on the concentration of the nucleoside that in turn may depend on neuronal firing activity. This adds a novel conceptual way to understand the fundamental role of astrocytes at tripartite synapses.

Acknowledgments We acknowledge the technical help obtained from Jasmina Jiménez (Molecular Neurobiology laboratory, Barcelona University). This study was supported by Fundação para a Ciência e a

Tecnologia (FCT) project grants, COST B30 action, grants from Spanish Ministerio de Ciencia y Tecnología (SAF2008-03229-E, SAF2008-00146), and funds from PRIN and Università Politecnica delle Marche (to F.C.). PJM is a Ramón y Cajal Fellow. SC-F is in receipt of an FCT fellowship (SFRH/BD/38099/2007).

References

1. Hamilton N, Attwell D (2010) Do astrocytes really exocytose neurotransmitters? Nat Rev Neurosci 11:227–238
2. Krnjevic K, Schwartz S (1967) The action of γ-aminobutyric acid on cortical neurons. Exp Brain Res 3:320–326
3. Artola A, Singer W (1987) Long-term potentiation and NMDA receptors in rat visual cortex. Nature 330:649–652
4. Blatow M, Rozov A, Katona I, Hormuzdi SG, Meyer AH, Whittington MA, Caputi A, Monyer H (2003) A novel network of multipolar bursting interneurons generates theta frequency oscillations in neocortex. Neuron 38:805–817
5. Minelli A, Brecha NC, Karschin C, DeBiasi S, Conti F (1995) GAT-1, a high-affinity GABA plasma membrane transporter, is localized to neurons and astroglia in the cerebral cortex. J Neurosci 15:7734–7746
6. Minelli A, DeBiasi S, Brecha NC, Conti F (1996) GAT-3, a high affinity GABA plasma membrane transporter, is localized exclusively to astrocytic processes in the cerebral cortex. J Neurosci 16:6255–6264
7. Hertz L, Schousboe A (1987) Primary cultures of GABAergic and glutamatergic neurons as model systems to study neurotransmitter functions: I. Differentiated cells. In: Model systems of development and aging of the nervous system. Giacobini E (eds). M Nijhoff Publ Com, Boston, pp 19–31
8. Fredholm BB, IJzerman AP, Jacobson KA, Klotz KN, Linden J (2001) International Union of Pharmacology. XXV. Nomenclature and classification of adenosine receptors. Pharmacol Rev 53:527–552
9. Correia-de-Sá P, Ribeiro JA (1994) Tonic adenosine A2A receptor activation modulates nicotinic autoreceptor function at the neuromuscular junction. Eur J Pharmacol 271:349–355
10. Cunha RA, Johansson B, van der Ploeg I, Sebastião AM, Ribeiro JA, Fredholm BB (1994) Evidence for functionally important adenosine A2a receptors in the rat hippocampus. Brain Res 649:208–216
11. Lopes LV, Cunha RA, Ribeiro JA (1999) Cross talk between A(1) and A(2A) adenosine receptors in the hippocampus and cortex of young adult and old rats. J Neurophysiol 82:3196–3203
12. Sebastião AM, Ribeiro JA (2000) Fine-tuning neuromodulation by adenosine. Trends Pharmacol Sci 21:341–346
13. Ciruela F, Casadó V, Rodrigues RJ, Luján R, Burgueño J, Canals M, Borycz J, Rebola N, Goldberg SR, Mallol J, Cortés A, Canela EI, López-Giménez JF, Milligan G, Lluis C, Cunha RA, Ferré S, Franco R (2006) Presynaptic control of striatal glutamatergic neurotransmission by adenosine A_1–A_{2A} receptor heteromers. J Neurosci 26:2080–2087
14. Ferré S, Navarro G, Casadó V, Cortés A, Mallol J, Canela EI, Lluís C, Franco R (2010) G protein-coupled receptor heteromers as new targets for drug development. Prog Mol Biol Transl Sci 91:41–52
15. Orru M, Bakešová J, Brugarolas M, Quiroz C, Beaumont V, Goldberg SR, Lluís C, Cortés A, Franco R, Casadó V, Canela EI, Ferré S (2011) Striatal pre- and postsynaptic profile of adenosine A(2A) receptor antagonists. PLoS One 6:e16088
16. Canals M, Marcellino D, Fanelli F, Ciruela F, de Benedetti P, Goldberg SR, Neve K, Fuxe K, Agnati LF, Woods AS, Ferré S, Lluís C, Bouvier M, Franco R (2003) Adenosine A2A-dopamine D2 receptor-receptor heteromerization: qualitative and quantitative assessment by fluorescence and bioluminescence energy transfer. J Biol Chem 278:46741–46749
17. Ciruela F, Burgueño J, Casadó V, Canals M, Marcellino D, Goldberg SR, Bader M, Fuxe K, Agnati LF, Lluis C, Franco R, Ferré S, Woods AS (2004) Combining mass spectrometry and pull-down techniques for the study of receptor heteromerization. Direct epitope-epitope electrostatic interactions between adenosine A2A and dopamine D2 receptors. Anal Chem 76:5354–5363
18. Sarrió S, Casadó V, Escriche M, Ciruela F, Mallol J, Canela EI, Lluis C, Franco R (2000) The heat shock cognate protein hsc73 assembles with A(1) adenosine receptors to form functional modules in the cell membrane. Mol Cell Biol 20:5164–5174
19. Schröder R, Janssen N, Schmidt J, Kebig A, Merten N, Hennen S, Müller A, Blättermann S, Mohr-Andrä M, Zahn S, Wenzel J, Smith NJ, Gomeza J, Drewke C, Milligan G, Mohr K, Kostenis E (2010) Deconvolution of complex G protein-coupled receptor signaling in live cells using dynamic mass redistribution measurements. Nat Biotechnol 28:943–949
20. Vaz SH, Jorgensen TN, Cristovão-Ferreira S, Duflot S, Ribeiro JA, Gether U, Sebastião AM (2011) Brain-derived neurotrophic factor (BDNF) enhances GABA transport by modulating the trafficking of GABA transporter-1 (GAT-1) from the plasma membrane of rat cortical astrocytes. J Biol Chem 286:40464–40476
21. Ferrada C, Moreno E, Casadó V, Bongers G, Cortés A, Mallol J, Canela EI, Leurs R, Ferré S, Lluís C, Franco R (2009) Marked changes in signal transduction upon heteromerization of dopamine D1 and histamine H3 receptor. Br J Pharmacol 157:64–75
22. Moreno E, Hoffmann H, Gonzalez-Sepúlveda M, Navarro G, Casadó V, Cortés A, Mallol J, Vignes M, McCormick PJ, Canela EI, Lluís C, Moratalla R, Ferré S, Ortiz J, Franco R (2011) Dopamine D1-histamine H3 receptor heteromers provide a selective link to MAPK signaling in GABAergic neurons of the direct striatal pathway. J Biol Chem 286:5846–5854
23. Ferré S, Baler R, Bouvier M, Caron MG, Devi LA, Durroux T, Fuxe K, George SR, Javitch JA, Lohse MJ, Mackie K, Milligan G, Pfleger KD, Pin JP, Volkow ND, Waldhoer M, Woods AS, Franco R (2009) Building a new conceptual framework for receptor heteromers. Nat Chem Biol 5:131–134
24. Rashid AJ, So CH, Kong MM, Furtak T, El-Ghundi M, Cheng R, O'Dowd BF, George SR (2007) D1-D2 dopamine receptor heterooligomers with unique pharmacology are coupled to rapid activation of Gq/11 in the striatum. Proc Natl Acad Sci USA 104:654–659
25. Gill DM, Meren R (1978) ADP-ribosylation of membrane proteins catalyzed by cholera toxin: Basis of the activation of adenylate cyclase. Proc Natl Acad Sci USA 75:3050–3054
26. Bokoch GM, Gilman AG (1984) Inhibition of receptor-mediated release of arachidonic acid by pertussis toxin. Cell 39:301–308
27. Smith RJ, Sam LM, Justen JM, Bundy GL, Bala GA, Bleasdale JE (1990) Receptor-coupled signal transduction in human polymorphonuclear neutrophils: effects of a novel inhibitor of phospholipase C-dependent processes on cell responsiveness. J Pharmacol Exp Ther 253:688–697
28. Wang LY, Salter MW, MacDonald JF (1991) Regulation of kainate receptors by cAMP-dependent protein kinase and phosphatases. Science 253:1132–1135
29. Awad JA, Johnson RA, Jakobs KH, Schultz G (1983) Interactions of forskolin and adenylate cyclase. Effects on substrate kinetics and protection against inactivation by heat and *N*-ethylmaleimide. J Biol Chem 258:2960–2965
30. Xiong L, Shuhendler AJ, Rao J (2012) Self-luminescing BRET-FRET near-infrared dots for in vivo lymph-node mapping and tumour imaging. Nat Commun 3:1193
31. Jordan BA, Trapaidze N, Gomes I, Nivarthi R, Devi LA (2001) Oligomerization of opioid receptors with beta 2-adrenergic

receptors: a role in trafficking and mitogen-activated protein kinase activation. Proc Natl Acad Sci U S A 98:343–348
32. Pfeiffer M, Kirscht S, Stumm R, Koch T, Wu D, Laugsch M, Schröder H, Höllt V, Schulz S (2003) Heterodimerization of substance P and mu-opioid receptors regulates receptor trafficking and resensitization. J Biol Chem 278:51630–51637
33. Smith NJ, Milligan G (2010) Allostery at G protein-coupled receptor homo- and heteromers: uncharted pharmacological landscapes. Pharmacol Rev 62:701–725
34. Han Y, Moreira IS, Urizar E, Weinstein H, Javitch JA (2009) Allosteric communication between protomers of dopamine class A GPCR dimers modulates activation. Nat Chem Biol 5:688–695
35. Ribeiro JA, Sebastião AM (1987) On the role, inactivation and origin of endogenous adenosine at the frog neuromuscular junction. J Physiol 384:571–585
36. Cunha RA, Vizi ES, Ribeiro JA, Sebastião AM (1996) Preferential release of ATP and its extracellular catabolism as a source of adenosine upon high- but not low-frequency stimulation of rat hippocampal slices. J Neurochem 67:2180–2187
37. Lovatt D, Xu Q, Liu W, Takano T, Smith NA, Schnermann J, Tieu K, Nedergaard M (2012) Neuronal adenosine release, and not astrocytic ATP release, mediates feedback inhibition of excitatory activity. Proc Natl Acad Sci U S A 109:6265–6270
38. Lee HU, Yamazaki Y, Tanaka KF, Furuya K, Sokabe M, Hida H, Takao K, Miyakawa T, Fujii S, Ikenaka K (2013) Increased astrocytic ATP release results in enhanced excitability of the hippocampus. Glia 61:210–224
39. Fields RD, Burnstock G (2006) Purinergic signalling in neuron–glia interactions. Nat Rev Neurosci 7:423–436
40. Klotz KN, Hessling J, Hegler J, Owman C, Kull B, Fredholm BB, Lohse MJ (1998) Comparative pharmacology of human adenosine receptor subtypes—characterization of stably transfected receptors in CHO cells. Naunyn Schmiedebergs Arch Pharmacol 357:1–9
41. Linden J, Thai T, Figler H, Jin X, Robeva AS (1999) Characterization of human A(2B) adenosine receptors: radioligand binding, western blotting, and coupling to G(q) in human embryonic kidney 293 cells and HMC-1 mast cells. Mol Pharmacol 56:705–713
42. Ongini E, Dionisotti S, Gessi S, Irenius E, Fredholm BB (1999) Comparison of CGS 15943, ZM 241385 and SCH 58261 as antagonists at human adenosine receptors. Naunyn-Schmiedeberg's Arch Pharmacol 359:7–10
43. Ji XD, Jacobson KA (1999) Use of the triazolotriazine [3H]ZM 241385 as a radioligand at recombinant human A2B adenosine receptors. Drug Des Discov 16:217–226